The Oncologist®

Imaging in Radiation Oncology: A Perspective

LAURA A. DAWSON, CYNTHIA MÉNARD

Radiation Medicine Program, Princess Margaret Hospital, University of Toronto, Toronto, Ontario, Canada

ABSTRACT

An inherent goal of radiation therapy is to deliver enough dose to the tumor to eradicate all cancer cells or to palliate symptoms, while avoiding normal tissue injury. Imaging for cancer diagnosis, staging, treatment planning, and radiation targeting has been integrated in various ways to improve the chance of this occurring. A large spectrum of imaging strategies and technologies has evolved in parallel to advances in radiation delivery. The types of imaging can be categorized into offline imaging (outside the treatment room) and online imaging (inside the treatment room, conventionally termed image-guided radiation therapy). The direct integration of images in the radiotherapy planning process (physically or computationally) often entails trade-offs in imaging performance. Although such compromises may be acceptable given specific clinical objectives, general requirements for imaging performance are expected to increase as paradigms for radiation delivery evolve to address underlying biology and adapt to radiation responses. This paper reviews the integration of imaging and radiation oncology, and discusses challenges and opportunities for improving the practice of radiation oncology with imaging. *The Oncologist* 2010;15: 338–349

INTRODUCTION

Shortly after the discovery of the x-ray in 1895, the potential therapeutic benefits of the x-ray and possible toxicities were realized. More than a century later, we continue to struggle with how to balance the intensity of cancer treatment toward increasing the chance of cure with the potential for normal tissue toxicity. Imaging has improved our understanding of the complexities of cancer biology, cancer diagnosis, staging, and prognosis, and it is an essential component of present-day radiation oncology practice. Progress in radiation oncology has occurred in parallel to advances in imaging.

One advance in radiation oncology relates to x-ray energy: from orthovoltage, with high skin doses, to megavoltage (MV), associated with skin sparing, facilitating treatment of central tumors. The integration of computed tomography (CT) imaging in the radiation process allowed the benefits of high-energy radiation to be exploited. CT imaging allows better knowledge of the target volume and critical normal organ position, and it serves as a platform upon which three-dimensional (3D) dose calculations can be made, such that the dose distribution throughout the entire irradiated volume may be
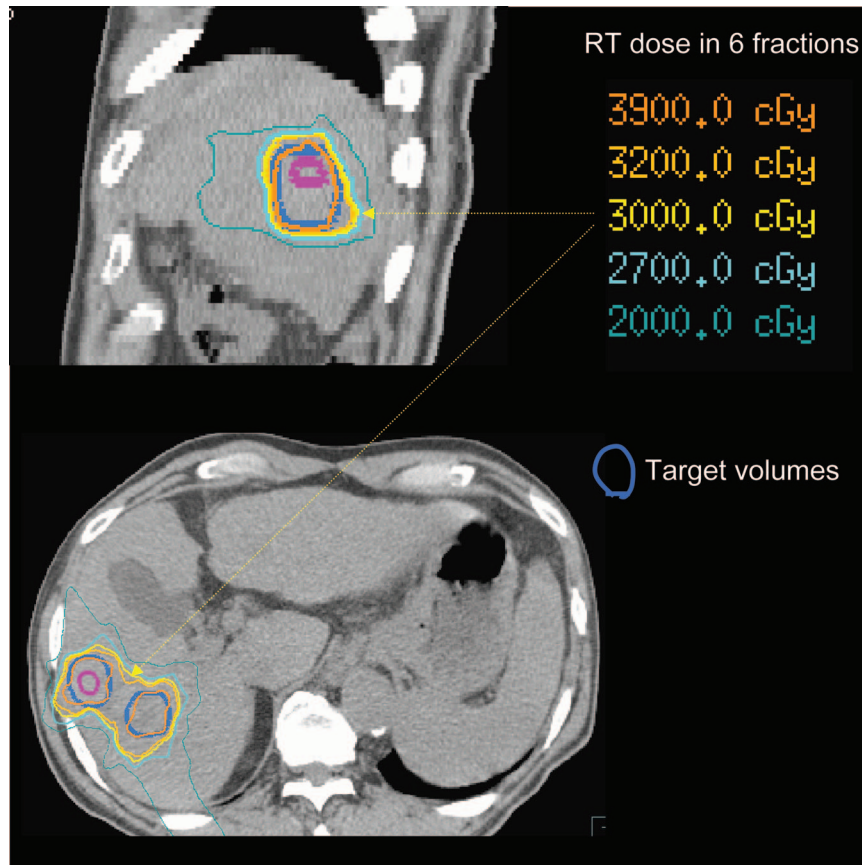
Figure 1. Radiation therapy (RT) dose distribution, demonstrating high doses tightly conforming to the target liver metastases volumes (shown in thick blue contours).

displayed. Only with this image-based process could radiation field apertures be customized to conform to an individual patient's target volumes (i.e., conformal radiation therapy [CRT]). Figure 1 shows an example of a CRT plan for a patient with liver metastases, in which the high doses tightly conform to the target volumes. 3D displays of target volumes and normal tissues are a prerequisite to more complex planning, for which the desired dose distribution is defined and computer-aided automated optimization is used to determine the beam fluence intensities associated with optimal dose distributions (i.e., intensity-modulated radiation therapy [IMRT]) (Fig. 2). An example of how advances in planning have improved patient outcomes is in head and neck cancer, for which sparing of the dose to the salivary glands has led to preserved salivary function and better quality of life in these patients [1].

In addition to anatomical and structural imaging, imaging more than anatomy is becoming established in cancer care. The ability to spatially measure biological, metabolic, or physiological processes provides exciting opportunities for radiation therapy (RT), a therapeutic modality that fundamentally performs best at the convergence of biology and physics. Such advanced imaging performance may enable radiation delivery to account for an individual's variability in tumor biology in a spatial- and time-responsive manner. Similarly, functional imaging can inform on normal tissue function, so that it can be considered in RT plan development, to better preserve the most functional portions of normal tissues.

The integration of images in the RT planning process often entails trade-offs in imaging performance, because of inherent limitations of integrated imaging and radiation treatment systems and/or the desire to minimize the cumulative dose delivered to patients from the frequent imaging required during a course of RT. Such compromises may be acceptable for some specific clinical objectives (e.g., reduction in geometric errors), but the requirements for imaging performance (including spatial resolution and imaging contrast) are expected to increase as biology is considered in RT planning and response monitoring. Figure 3 illustrates this balance between imaging performance and integration with the RT process.

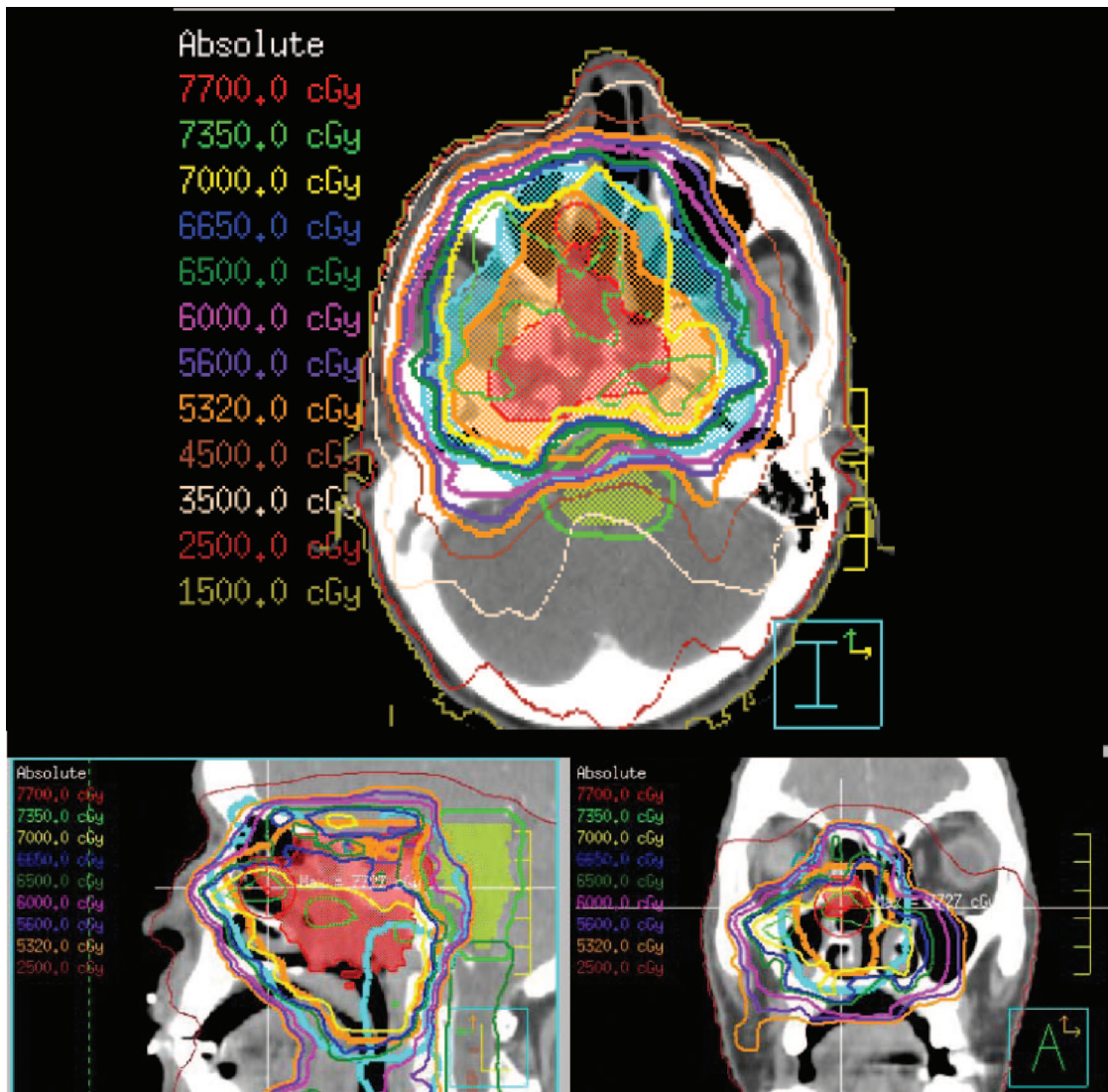The outer circle represents the fundamental objectives

Figure 2. Intensity-modulated radiation therapy plan for a patient with a T4N1M0 nasopharyngeal carcinoma, adjacent to critical normal tissues (e.g., brainstem and optic tissues), treated to 70 Gy in 35 fractions.

of RT. Trade-offs among geometric integrity (for geometric targeting and serial/multimodality registration accuracy), tissue contrast (for target delineation, dose selection, and response assessment), and spatial resolution (for high-precision delineation of subtarget boundaries) must be considered and goals must be prioritized, because concurrent state-of-the-art spatial and temporal resolution is not clinically feasible or time efficient. As volumetric image guidance during radiation delivery begins to predominate over conventional external landmark guidance techniques, the focus on geometry (e.g., maintaining patient position with rigid immobilization) is projected to diminish in contrast to the emphasis on quantitative, high-performance imaging with effective registration methods that may be used to position patients for therapy. The future research in this direction should target implementation of oncology-specific imaging methods that can increase the quality and performance of imaging in a manner specific to the goals of RT.

RT PROCESS

The primary decisions that radiation oncologists make daily are to decide who to treat, what to treat, what to avoid, and how to deliver the intended doses safely. Imaging is considered in each of these decisions. Although the steps described in sequence below often occur simultaneously, they feed back to each other. Predictions about uncertainties and response in a specific patient can be made from experience in treating a population of similar patients or as more is learned about the patients themselves (e.g., with imaging obtained during therapy).
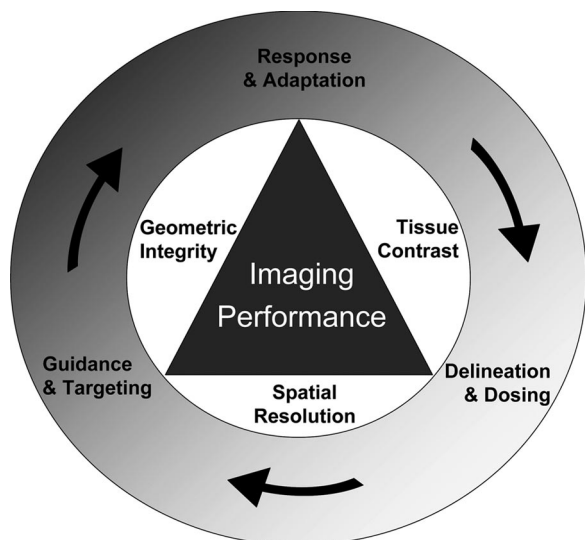
Figure 3. Diagram depicting the importance of optimizing imaging performance based on the fundamental objectives of radiotherapy (outer circle). Trade-offs among geometric integrity, tissue contrast, and spatial resolution must be considered when designing time-efficient image acquisition protocols.

Decision to Treat

As imaging improves, our ability to stage patients, detect occult metastatic disease, and better select patients for RT improves. For example, fluorodeoxyglucose positron emission tomography (FDG-PET) has improved staging in non-small cell lung cancer (NSCLC), which can impact treatment decision making. In one study, PET detected occult metastases and prevented unnecessary surgery in 20% of patients with suspected localized NSCLC [2]. Better staging will help to define the most appropriate patients who may benefit from RT.

RT Patient Model

CRT and IMRT plans are generally based on a CT image obtained prior to RT delivery, to create a patient model for planning. Because the CT "sample" of the patient is usually acquired over 30–60 seconds on one instance, it is unlikely to represent the patient and target geometry over the course of RT. Thus, it is desirable to enable serial and or multimodality imaging in the RT planning process. Greater use of imaging in patients receiving RT (e.g., with repeat CT or magnetic resonance imaging [MRI] scans) has increased awareness of the geometric uncertainties that may occur during a course of RT. Furthermore, the integration of multimodality imaging in the patient model is beneficial because different imaging modalities can be complimentary in the anatomical and functional information provided. For example, MRI depicts soft tissue structure better than CT, and has particular utility in aiding in target delineation in some head and neck cancers, brain tumors, sarcomas, and

soft tissue targets in the abdomen and pelvis. Its integration with CT to augment the RT patient model is increasingly becoming an essential step in the process of modern radiation treatment planning [3–7].

Patients have historically been imaged in the treatment position, which involves a flat tabletop and a customized cradle or mask to attempt to keep the patient in the same position during a course of RT. The driving motivation for such strict (and often prohibitive) requirements on patient position during imaging for RT planning stems from an era prior to online image guidance, in which targeting accuracy relied exclusively on recreating the geometry of the patient model through immobilization devices and external references. A second motivation in the modern era is to improve the accuracy of multimodality or serial image registration, in the absence of robust deformable registration software tools.

With image-guided radiation therapy (IGRT) and future robust deformable image registration tools [8, 9], more day-to-day (or crossmodality) variations in position may be permitted, which may improve patient comfort and stability, translating to less variation in position during radiation delivery. This may also improve imaging performance (tissue contrast and spatial resolution) by applying imaging devices, such as receiver MRI coils, closer to the patient.

Target Delineation

How to define the gross tumor volume and volumes at risk for containing microscopic disease (clinical target volumes [CTVs]) is not an easy task. Different imaging tools demonstrate inherently different representations of the tumor, as shown in Figure 4. Because the tumor stem cells required to be eradicated cannot yet be imaged in vivo, a model of the tissue target to be eradicated needs to be developed. Most often, all gross disease (or visible enhancing tumor) is chosen as the target volume to be irradiated to high doses, but pathological–radiological correlative studies are required to determine which imaging modality may be best correlated with pathological gross tumor [10].

Delineation of microscopic disease is also challenging, and for the most part, in vivo imaging resolution is not sufficient to see microscopic foci of tumor. Conglomerates of <100,000 cancer cells cannot reliably be imaged. Imaging surrogates may inform us about volumes at risk for microscopic disease involvement. Pathologic–radiologic correlative studies can also help in CTV definition. For example, the outer enhancing rim around liver metastases on venous-phase CT scans may represent vascular changes around the gross tumor, a volume that is itself at risk for microscopic extension from the liver metastases. How we understand and define the spatial boundaries and dose objectives of tar-
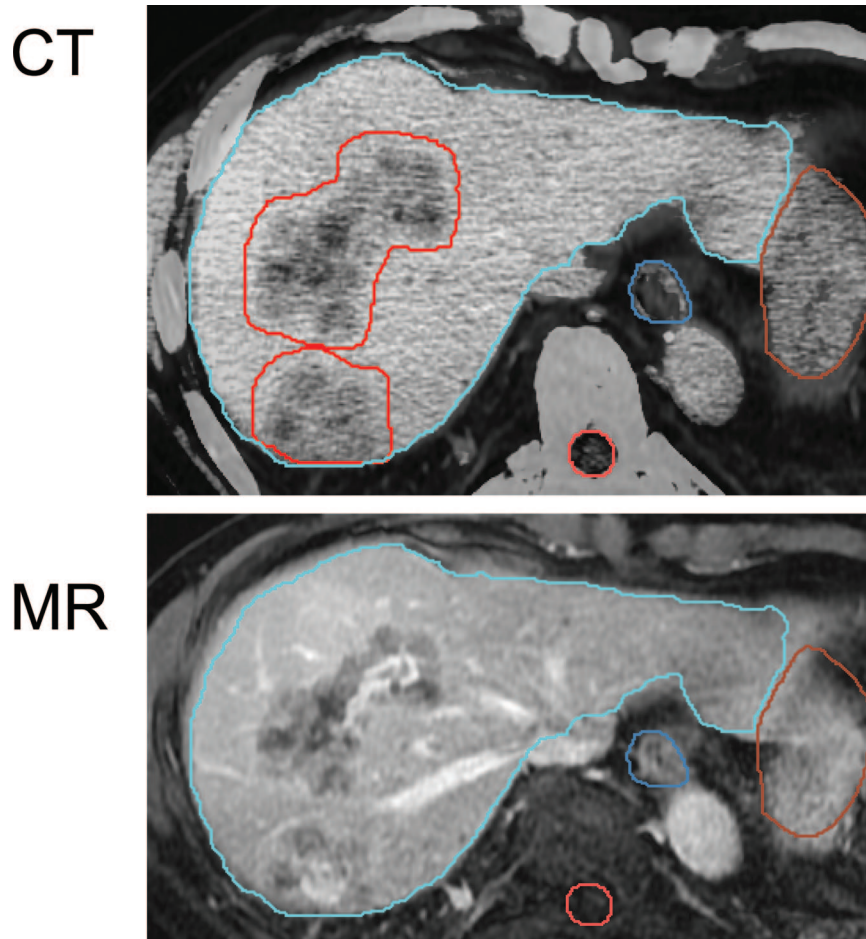
Figure 4. Multimodality contrast imaging to aid in liver metastasis delineation. Both computed tomography (CT) and magnetic resonance (MR) imaging are done in an exhale breathhold to minimize differences in the liver shape and aid in fusion. The liver contour from the planning CT (in blue) is overlaid on the MR image, demonstrating excellent liver-to-liver registration.

gets for RT remain fundamentally unanswered, and mandate judicious investigation. High-performance imaging, in the context of high-precision radiation delivery, will enable this important research.

Motion Assessment

Despite interventions to immobilize patients, residual uncertainties in the position of the tumor and normal tissues persist. The conventional method to account for these uncertainties is to increase the irradiated volume around the tumor to ensure that the tumor receives the intended dose (referred to as a planning target volume [PTV]). The magnitude of the PTV around the tumor site, patient body habitus, position, immobilization, and motion management strategy determine the image guidance strategy used.
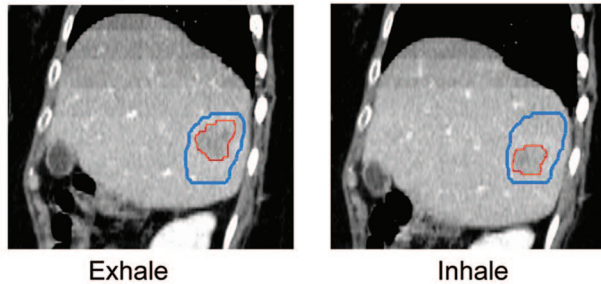
Tumor and normal tissue motion resulting from breathing can be substantial (up to 3 cm) [11]. Motion needs to be reduced and/or considered at the time of RT planning to ensure that the tumor isn't missed. Before motion manage-

ment can be implemented, knowledge of an individual cancer patient's breathing motion is required. Breathing motion can be measured using kV fluoroscopy, cine MR, or respiratory-sorted CT (or 4DCT) (Fig. 5). With 4DCT, multiple representations at different breathing phases can be used in the patient model to represent geometric changes that may occur during breathing. With more imaging in the treatment room, variability in the amplitude of motion and other changes (e.g., shifts in tumor position relative to vertebral bodies) can be quantified [12]. Imaging obtained in the treatment room can also inform on population setup error, and how it varies depending on the type of immobilization used, length of treatment delivery, etc. [13].

Determining Planned Doses

The appropriate doses to be delivered to the targets and normal tissues are obtained from clinical trials, ideally prospective trials that compare different doses with local control and normal tissue toxicity. There is much uncer-
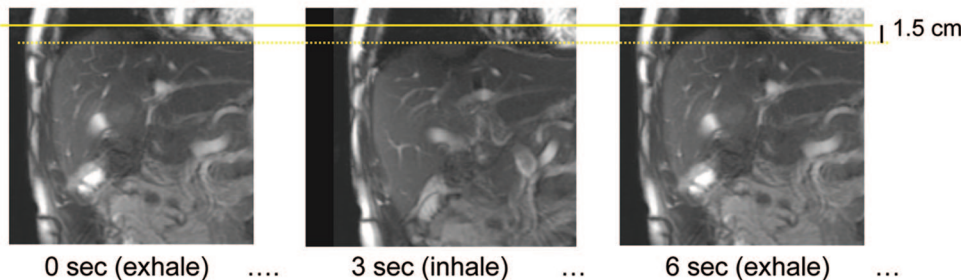
Figure 5. Imaging for motion assessment of liver cancer to determine the margin around the tumor required to be irradiated to account for breathing motion. **(A):** Respiratory-correlated computed tomography (CT) scan showing tumor (red contour) in the exhale and inhale phases of CT. The blue contour shows the volume to be irradiated to ensure the tumor is irradiated in all phases of respiration. **(B):** Coronal cine magnetic resonance (MR) images showing the change in liver position from the exhale to the inhale phases.

tainty in the actual doses required to control many tumors and in our understanding of the partial volume tolerance of many normal tissues to irradiation. This is partially because much uncertainty has existed historically in the actual doses delivered to patients.

Because image-guidance technologies provide confidence in dose placement, there is less uncertainty in delivered doses with IGRT and less variability in delivered doses across a population. Thus, in future clinical trials for which IGRT is mandated, understanding of dose–toxicity relationships should improve and the benefits of dose escalation, hypofractionation, and combined modality therapy should be easier to measure, because the accuracy and precision of RT should be improved with IGRT.

IGRT

Historically, patients were positioned for RT by inferring the location of the internal anatomy from the surface anatomy. However, the internal anatomy is not generally well correlated with the surface anatomy, providing a need for imaging at the time of RT delivery. Furthermore, large PTV margins to account for geometric uncertainties and organ motion are undesirable because they may increase the risk for normal tissue toxicity. A better strategy is to measure changes during the RT course with frequent imaging ob-

tained in the treatment room, and to reduce residual uncertainties by repositioning the patient (e.g., with IGRT).

Images produced using the MV treatment x-ray beam itself have been used to image internal anatomy to position patients or to verify the position, following setup, with the external anatomy. Machine- and room-mounted kV x-ray tubes and detectors have also been used for this purpose. kV fluoroscopy has been used to image radio-opaque markers prior to each radiation fraction [14, 15], or throughout radiation delivery [16]. The combination of fluoroscopy and markers enables real-time tumor tracking [16], in which radiation delivery only occurs when the markers (surrogates for the target volume) are in a predefined volume. Other image-based strategies to account for tumor motion include tracking the tumor with moving collimators [17] or moving the couch or the accelerator to follow the tumor (e.g., Cyber-Knife; Accuray Inc., Sunnyvale, CA [18–20]). Inserted radio-opaque markers have been used to localize prostate [21, 22], lung [16], pancreatic [19], paraspinal [19] and liver [23, 24] cancers.

In-room volumetric imaging has been developed to allow soft tissues to be localized at the time of RT delivery. Ultrasound [25–30] and in-room CT scanners [31–33] were the first volumetric imaging strategies used in the treatment room (e.g., Primatrom; Siemens, Concord, CA and ExaCT;
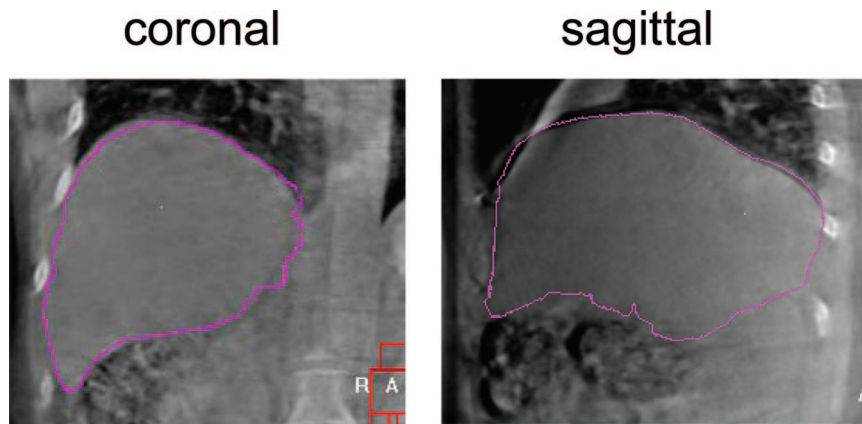
coronal   sagittal

Figure 6. Example of verification imaging (kilovoltage cone beam computed tomography [CT]) obtained in the radiation therapy treatment room, used to position a patient with liver cancer prior to conformal radiation therapy delivery. The pink contour, representing where the liver should be positioned (obtained from the planning CT), is overlaid on the verification cone beam CT image.

Varian Medical Systems, Palo Alto, CA) [34, 35]. Helical MV CT scans can be obtained using an integrated treatment unit (Tomotherapy, Madison, WI) that allows the MV treatment beam to rotate around the patient while the couch moves, creating volumetric MV images [36–40]. kV cone-beam CT systems integrate a kV tube and a flat panel detector mounted on a linear accelerator (e.g., Synergy; Elekta Oncology, Stockholm, Sweden; On Board Imager; Varian Medical Systems, Palo Alto, CA; Artiste; Siemens, Concord, CA) [41] to obtain a reconstruction from a series of 2D radiographs acquired over 30–240 seconds as the gantry rotates around the patient [42–50]. Ring-gantry systems have also been developed to offer cone-beam CT imaging as well as a tilting treatment head for tumor tracking with kV fluoroscopy [51]. MR-guided RT systems are also being developed [52].

With in-room imaging systems, images acquired immediately before or during RT delivery can be compared with reference images (from the planning CT) to better position the patient, as show in Figure 6. This can occur using manual or automated image registration. With image guidance, weight loss, tumor shrinkage, or organ deformation may be visualized, and the doses delivered in the presence of such changes can be measured. Sometimes these changes may trigger a need for replanning, referred to as adaptive RT [53, 54].

Response Monitoring
The development of early imaging surrogates for tumor control and normal tissue toxicity are of interest, because they may allow a change in treatment to occur before completion of the prescribed therapy, maximizing the patient's therapeutic ratio. Measurable responses in tissue structure often occur late in the course of RT, at which time options

for adapting therapeutic interventions are limited. Functional imaging has the potential to detect individual tumor's response to RT earlier in the course of treatment. One of the first examples of this potential was observed in patients with malignant gliomas, whereby changes in the apparent water diffusion coefficient measured with MRI midway through a course of RT were highly predictive of outcome [55]. This exciting field of research continues to pursue the discovery of imaging biomarkers that capture measurable and early response to RT, predictive of clinical outcome, and that will guide adaptive strategies in therapy.

The impact of the dose delivered on functional imaging surrogates, tumor control, and regional normal tissue injury requires a detailed knowledge of the 3D dose distribution. Thus, mapping back where recurrences occur relative to the treatment plan and baseline images can be informative about how changes in RT planning could reduce the risk for future recurrences. Furthermore, knowledge of the doses associated with normal tissue subregional injury may help in predicting organ injury from RT. These tasks require deformable image registration for the most accurate mapping of dose to spatial imaging change.

ILLUSTRATING THE BENEFITS OF IMAGING IN RT FOR PROSTATE CANCER

Example 1: External-Beam RT
In regard to prostate cancer, when patients are set up for RT using skin marks and room lasers to position them, offsets in the prostate position >10 mm have been seen, and these are more common in patients with a larger body surface area, providing strong rationale for IGRT to reduce setup error [56]. Perhaps the historic challenges in demonstrating the benefits of RT in prostate cancer and the unclear evi-

dence for the use of pelvic irradiation for prostate cancer relate in part to the fact that the intended doses to the prostate were not delivered as planned in some patients.

The potential benefits of IGRT in prostate cancer have been modeled. An average increase in dose of 13% was predicted with the use of IGRT, with the same risk for rectal toxicity [57], with larger gains for some patients. Clinical data also support superior outcomes with IGRT for prostate cancer. Rectal size at the time of RT planning in prostate cancer patients treated without IGRT was found to be a prognostic factor for prostate-specific antigen (PSA)-free survival in one series [58]. The 6-year PSA-free survival rates of patients with full and empty rectums were 65% and 80%, respectively (hazard ratio, 3.89; 95% confidence interval, 1.58–9.59; $p = .003$). This change in outcome is likely related to the fact that a distended rectum at planning (because of gas or feces) is less likely to be distended during treatment, and the prostate may move posteriorly during RT, out of the high-dose volume. This hypothesis is supported by the fact that the rectal volume at planning was not a prognostic factor in studies of prostate cancer in which IGRT was mandated [59].

Example 2: Brachytherapy

The history of prostate brachytherapy illustrates a clear benefit to image guidance [60, 61]. Since Pasteau's publication in 1913 [62], describing insertion of a radium capsule into the prostatic urethra to treat carcinoma of the prostate, various techniques have been employed with unsatisfactory results. In 1917, Barringer first performed transperineal brachytherapy under transrectal tactile guidance [63]. Decades later, in the early 1970s, Whitmore et al. [64] described open retropubic implantation guided by both direct intraoperative visualization of the prostate and transrectal palpation. Poor long-term outcomes were attributed to freehand source placement and inadequate dosimetry. In fact, dosimetry was largely calculated from radiographs, assuming that the target tissue was accurately encompassed by the implant [65]. The advent of transrectal ultrasound (TRUS), which permitted direct visualization of needles in relation to prostatic boundaries [66], revolutionized brachytherapy for prostate cancer. Prostate brachytherapy is now considered a standard care therapeutic option for the majority of patients with newly diagnosed prostate cancer.

Disappointment with early historical results and the subsequent success of permanent seed prostate brachytherapy with the advent of TRUS and image-based planning demonstrate the impact of image guidance on clinical outcomes for prostate cancer. Greater freedom from biochemical failure has been shown with technical maturation and the implementation of CT-based postbrachytherapy plan-

ning dosimetry [67]. Most modern publications in this field demonstrate better dosimetry with further advances in image guidance [68–78]. However, the relationship between dosimetry and clinical outcomes has yet to be fully defined. It is important to recognize that the accuracy of dose reporting is highly dependent on the accuracy of target delineation, and uncertainties in this regard may have contributed to inconsistencies in the observed dose–response relationship [79–81]. This problem also holds true for our understanding of the relationship between critical organ dose and subsequent toxicity [82, 83]. Image guidance in prostate brachytherapy has evolved in recent decades from US to CT to MRI (Fig. 7).

OPPORTUNITIES IN IMAGING: DOSE-PAINTING EXAMPLE

Functional imaging modalities such as PET, single photon emission CT, and functional MRI are becoming more valuable for diagnosis, staging, describing the tumor and normal tissue biology, and assessing response. Variations in the tumor, the tumor microenvironment, or cellular phenotypes that may modulate the effect of radiation can now be mapped in 3D and over time. A simple example of functional imaging is ^{18}F-FDG-PET scanning, which may be used to measure glucose metabolism as a surrogate for tumor burden. Examples of other high-risk characteristics that may be measured by functional imaging include hypoxia, which can be measured using ^{18}F-fluoromisonidazole-PET, ^{60}Cu-diacetyl-bis N(4)-methyl-thiosemicarbazone (ATSM)-PET, or blood oxygen level–dependent imaging MRI, and proliferation, measured with ^{18}F-fluorothymine-PET. Other processes that may be imaged and quantified include clonogen density, angiogenesis, blood flow, vascular permeability, epidermal growth receptor expression, etc.

There is an opportunity to tailor RT plans for each patient to account for individual biological variations. Furthermore, because individual variability can be measured, there is the opportunity to tailor the radiation dose distribution to the variability in cellular or molecular processes, as measured using functional imaging. This has been referred to as theragnostic imaging, described by Bentzen as "a method by which the radiation dose can be delivered in the four dimensions of space and time to achieve the optimum outcome after radiation therapy" [84]. The feasibility of this approach—to increase the intensity of the dose to high-risk tumor subregions—was demonstrated by Chao et al. [85], who used ^{62}Cu (II) ATSM-PET scans in head and neck cancer patients to measure tumor hypoxia and boosted the dose to hypoxic regions (from 70 Gy to 80 Gy in 35 fractions), without increasing the dose to normal tissues. Challenges with this theragnostic approach include verifying that the
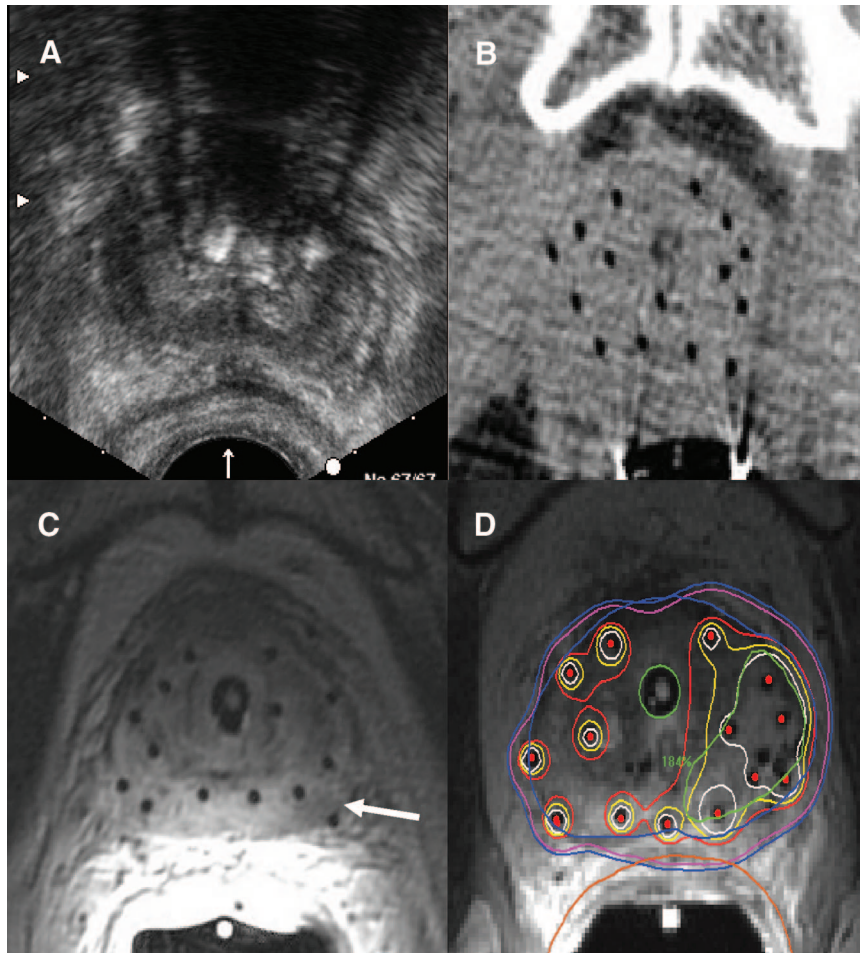
Figure 7. Images acquired after the placement of high-dose rate (HDR) brachytherapy catheters and prior to radiation delivery in one patient demonstrating the superiority of magnetic resonance imaging (MRI) in depicting both the catheters and prostatic anatomy. **(A):** Transrectal ultrasound. **(B):** Computed tomography. **(C):** MRI. The tumor visualized in the left peripheral zone (arrow) can be specifically targeted for dose intensification during brachytherapy planning **(D)**.

imaging measures the intended biologic process accurately, that the process is temporally stable, and that adaptive interventions are effective. Also, many of the functional imaging tools do not have sufficient spatial resolution, and artifacts exist, making selective boosting of high-risk tumor subvolumes or "painting by numbers" (voxel intensity–based dose boosting) not ready for large-scale trials. However, as the sensitivity and specificity (accuracy) of functional imaging improves, and the spatial resolution improves, the potential to "dose paint" becomes more real.

FUTURE: IMPROVED INTEGRATION OF IMAGING SCIENCE IN RADIATION ONCOLOGY

As imaging becomes increasingly integrated into the practice of radiation oncology, there is a need to develop a deeper understanding of the truth underlying the image. Our field must develop expertise in imaging science, such that the metric reported in a target voxel can be interpreted

in the context of technical biases and factors of biological origin that may or may not be relevant to the radiation objective. Radiation oncologists and imaging scientists must participate in the process of validating images at the clinical, histopathological, and molecular levels. A better understanding of both the tools and objectives of imaging in radiation oncology will likely have a high clinical impact.

An example of this potential contribution is a new emphasis on quantitative imaging, as opposed to qualitative diagnostic images interpreted largely for disease classification. The shift toward evidence-based medicine demands that outcomes be measurable, and imaging is intrinsically quantitative. Radiation oncology fundamentally understands the process of administering energy of a known quantity and distribution to a living organism. Measuring the energy that is emitted, transmitted, or reflected (i.e., imaging) lends itself to quantitative interpretation [86].

In the modern era of high-precision image-based RT, ra-

diation oncology departments need to invest in imaging. A stronger education on the fundamentals of imaging is required, at least with respect to tumor and normal tissue definition. This may be feasible through several means: by collaboration with imaging scientists and radiologists, by developing imaging expertise in radiation oncology through self-education (radiation oncologist), and by attracting imaging scientists into the field. At the very least, the formal imaging education in radiation oncology training programs needs to improve substantially. Radiation oncologists cannot move forward without considering imaging and how it impacts the radiation oncology process.

REFERENCES

1 Eisbruch A, Dawson LA, Kim HM et al. Conformal and intensity modulated irradiation of head and neck cancer: The potential for improved target irradiation, salivary gland function, and quality of life. Acta Otorhinolaryngol Belg 1999;53:271–275.

2 van Tinteren H, Hoekstra OS, Smit EF et al. Effectiveness of positron emission tomography in the preoperative assessment of patients with suspected non-small-cell lung cancer: The PLUS multicentre randomised trial. Lancet 2002;359:1388–1393.

3 Khoo VS, Joon DL. New developments in MRI for target volume delineation in radiotherapy. Br J Radiol 2006;79:S2–S15.

4 Haie-Meder C, Pötter R, Van Limbergen E et al. Recommendations from Gynaecological (GYN) GEC-ESTRO Working Group (I): Concepts and terms in 3D image based 3D treatment planning in cervix cancer brachytherapy with emphasis on MRI assessment of GTV and CTV. Radiother Oncol 2005;74:235–245.

5 Krempien RC, Daeuber S, Hensley FW et al. Image fusion of CT and MRI data enables improved target volume definition in 3D-brachytherapy treatment planning. Brachytherapy 2003;2:164–171.

6 Voroney JP, Brock KK, Eccles C et al. Prospective comparison of computed tomography and magnetic resonance imaging for liver cancer delineation using deformable image registration. Int J Radiat Oncol Biol Phys 2006;66:780–791.

7 Emami B, Sethi A, Petruzzelli GJ. Influence of MRI on target volume delineation and IMRT planning in nasopharyngeal carcinoma. Int J Radiat Oncol Biol Phys 2003;57:481–488.

8 Brock KK, Dawson LA, Sharpe MB et al. Application of a novel deformable image registration technique to facilitate classification, tracking and targeting of tumor and normal tissue. Int J Radiat Oncol Biol Phys 2004; 60:S227.

9 Kashani R, Hub M, Balter JM et al. Objective assessment of deformable image registration in radiotherapy: A multi-institution study. Med Phys 2008;35:5944–5953.

10 Geets X, Daisne JF, Tomsej M et al. Impact of the type of imaging modality on target volumes delineation and dose distribution in pharyngo-laryngeal squamous cell carcinoma: Comparison between pre- and per-treatment studies. Radiother Oncol 2006;78:291–297.

11 Langen KM, Jones DT. Organ motion and its management. Int J Radiat Oncol Biol Phys 2001;50:265–278.

12 Case RB, Sonke JJ, Moseley D et al. Inter- and intra-fraction variability in liver position in non-breath-hold stereotactic body radiotherapy. Int J Radiat Oncol Biol Phys 2009;75:302–308.

13 Velec M, Waldron J, O'Sullivan B et al. Cone beam CT assessment of inter- and intra-fraction setup error of two head and neck cancer thermoplastic masks. Int J Radiat Oncol Biol Phys 2009 (in press).

14 Dawson LA, Eccles C, Bissonnette JP et al. Accuracy of daily image guidance for hypofractionated liver radiotherapy with active breathing control. Int J Radiat Oncol Biol Phys 2005;62:1247–1252.

15 Balter JM, Brock KK, Litzenberg DW et al. Daily targeting of intrahepatic tumors for radiotherapy. Int J Radiat Oncol Biol Phys 2002;52:266–271.

16 Shirato H, Shimizu S, Kitamura K et al. Four-dimensional treatment planning and fluoroscopic real-time tumor tracking radiotherapy for moving tumor. Int J Radiat Oncol Biol Phys 2000;48:435–442.

17 Keall PJ, Joshi S, Vedam SS et al. Four-dimensional radiotherapy planning for DMLC-based respiratory motion tracking. Med Phys 2005;32:942–951.

18 Gerszten PC, Ozhasoglu C, Burton SA et al. Evaluation of CyberKnife frameless real-time image-guided stereotactic radiosurgery for spinal lesions. Stereotact Funct Neurosurg 2003;81:84–89.

19 Murphy MJ, Adler JR Jr, Bodduluri M et al. Image-guided radiosurgery for the spine and pancreas. Comput Aided Surg 2000;5:278–288.

20 Koong AC, Le QT, Ho A et al. Phase I study of stereotactic radiosurgery in patients with locally advanced pancreatic cancer. Int J Radiat Oncol Biol Phys 2004;58:1017–1021.

21 Balter JM, Lam KL, Sandler HM et al. Automated localization of the prostate at the time of treatment using implanted radiopaque markers: Technical feasibility. Int J Radiat Oncol Biol Phys 1995;33:1281–1286.

22 Schallenkamp JM, Herman MG, Kruse JJ et al. Prostate position relative to pelvic bony anatomy based on intraprostatic gold markers and electronic portal imaging. Int J Radiat Oncol Biol Phys 2005;63:800–811.

23 Balter JM, Dawson LA, Kazanjian S et al. Determination of ventilatory liver movement via radiographic evaluation of diaphragm position. Int J Radiat Oncol Biol Phys 2001;51:267–270.

24 Wu J, Haycocks T, Alasti H et al. Positioning errors and prostate motion during conformal prostate radiotherapy using on-line isocentre set-up verification and implanted prostate markers. Radiother Oncol 2001;61:127–133.

25 Van den Heuvel F, Powell T, Seppi E et al. Independent verification of ultrasound based image-guided radiation treatment, using electronic portal imaging and implanted gold markers. Med Phys 2003;30:2878–2887.

26 Mohan DS, Kupelian PA, Willoughby TR. Short-course intensity-modulated radiotherapy for localized prostate cancer with daily transabdominal ultrasound localization of the prostate gland. Int J Radiat Oncol Biol Phys 2000;46:575–580.

27 Kuban DA, Dong L, Cheung R et al. Ultrasound-based localization. Semin Radiat Oncol 2005;5:180–191.

28 Langen KM, Pouliot J, Anezinos C et al. Evaluation of ultrasound-based

prostate localization for image-guided radiotherapy. Int J Radiat Oncol Biol Phys 2003;57:635–644.

29 Fuss M, Salter BJ, Herman TS et al. External beam radiation therapy for hepatocellular carcinoma: Potential of intensity-modulated and image-guided radiation therapy. Gastroenterology 2004;127(suppl 1):S206–S217.

30 Artignan X, Smitsmans MH, Lebesque JV et al. Online ultrasound image guidance for radiotherapy of prostate cancer: Impact of image acquisition on prostate displacement. Int J Radiat Oncol Biol Phys 2004;59:595–601.

31 Court L, Rosen I, Mohan R et al. Evaluation of mechanical precision and alignment uncertainties for an integrated CT/LINAC system. Med Phys 2003;30:1198–1210.

32 Kuriyama K, Onishi H, Sano N et al. A new irradiation unit constructed of self-moving gantry-CT and linac. Int J Radiat Oncol Biol Phys 2003;55:428–435.

33 Onishi H, Kuriyama K, Komiyama T et al. A new irradiation system for lung cancer combining linear accelerator, computed tomography, patient self-breath-holding, and patient-directed beam-control without respiratory monitoring devices. Int J Radiat Oncol Biol Phys 2003;56:14–20.

34 Uematsu M, Fukui T, Shioda A et al. A dual computed tomography linear accelerator unit for stereotactic radiation therapy: A new approach without cranially fixated stereotactic frames. Int J Radiat Oncol Biol Phys 1996;35:587–592.

35 Cheng CW, Wong J, Grimm L et al. Commissioning and clinical implementation of a sliding gantry CT scanner installed in an existing treatment room and early clinical experience for precise tumor localization. Am J Clin Oncol 2003;26:e28–e36.

36 Mackie TR, Kapatoes J, Ruchala K et al. Image guidance for precise conformal radiotherapy. Int J Radiat Oncol Biol Phys 2003;56:89–105.

37 Groh BA, Siewerdsen JH, Drake DG et al. A performance comparison of flat-panel imager-based MV and kV cone-beam CT. Med Phys 2002;29:967–975.

38 Langen KM, Zhang Y, Andrews RD et al. Initial experience with megavoltage (MV) CT guidance for daily prostate alignments. Int J Radiat Oncol Biol Phys 2005;62:1517–1524.

39 Welsh JS, Bradley K, Ruchala KJ et al. Megavoltage computed tomography imaging: A potential tool to guide and improve the delivery of thoracic radiation therapy. Clin Lung Cancer 2004;5:303–306.

40 Langen KM, Meeks SL, Poole DO et al. The use of megavoltage CT (MVCT) images for dose recomputations. Phys Med Biol 2005;50:4259–4276.

41 Jaffray DA, Drake DG, Moreau M et al. A radiographic and tomographic imaging system integrated into a medical linear accelerator for localization of bone and soft-tissue targets. Int J Radiat Oncol Biol Phys 1999;45:773–789.

42 Oldham M, Létourneau D, Watt L et al. Cone-beam-CT guided radiation therapy: A model for on-line application. Radiother Oncol 2005;75:271–278.

43 Sonke JJ, Zijp L, Remeijer P et al. Respiratory correlated cone beam CT. Med Phys 2005;32:1176–1186.

44 Létourneau D, Martinez AA, Lockman D et al. Assessment of residual error for online cone-beam CT-guided treatment of prostate cancer patients. Int J Radiat Oncol Biol Phys 2005;62:1239–1246.

45 Jaffray DA. Emergent technologies for 3-dimensional image-guided radiation delivery. Semin Radiat Oncol 2005;15:208–216.

46 Godfrey DJ, Yin FF, Oldham M et al. Digital tomosynthesis with an on-board kilovoltage imaging device. Int J Radiat Oncol Biol Phys 2006;65:8–15.

47 Henry AM, Stratford J, McCarthy C et al. X-ray volume imaging in bladder radiotherapy verification. Int J Radiat Oncol Biol Phys 2006;64:1174–1178.

48 McBain CA, Henry AM, Sykes J et al. X-ray volumetric imaging in image-guided radiotherapy: The new standard in on-treatment imaging. Int J Radiat Oncol Biol Phys 2006;64:625–634.

49 Oelfke U, Tücking T, Nill S et al. Linac-integrated kV-cone beam CT: Technical features and first applications. Med Dosim 2006;31:62–70.

50 Li T, Xing L, Munro P et al. Four-dimensional cone-beam computed tomography using an on-board imager. Med Phys 2006;33:3826–3833.

51 Kamino Y, Takayama K, Kokubo M et al. Development of a four-dimensional image-guided radiotherapy system with a gimbaled x-ray head. Int J Radiat Oncol Biol Phys 2006;66:271–278.

52 Raaymakers BW, Raaijmakers AJ, Kotte AN et al. Integrating a MRI scanner with a 6 MV radiotherapy accelerator: Dose deposition in a transverse magnetic field. Phys Med Biol 2004;49:4109–4118.

53 Yan D, Lockman D, Martinez A et al. Computed tomography guided management of interfractional patient variation. Semin Radiat Oncol 2005;15:168–179.

54 Wu Q, Liang J, Yan D. Application of dose compensation in image-guided radiotherapy of prostate cancer. Phys Med Biol 2006;51:1405–1419.

55 Moffat BA, Chenevert TL, Lawrence TS et al. Functional diffusion map: A noninvasive MRI biomarker for early stratification of clinical brain tumor response. Proc Natl Acad Sci U S A 2005;102:5524–5529.

56 Millender LE, Aubin M, Pouliot J et al. Daily electronic portal imaging for morbidly obese men undergoing radiotherapy for localized prostate cancer. Int J Radiat Oncol Biol Phys 2004;59:6–10.

57 Ghilezan M, Yan D, Liang J et al. Online image-guided intensity-modulated radiotherapy for prostate cancer: How much improvement can we expect? A theoretical assessment of clinical benefits and potential dose escalation by improving precision and accuracy of radiation delivery. Int J Radiat Oncol Biol Phys 2004;60:1602–1610.

58 de Crevoisier R, Tucker SL, Dong L et al. Increased risk of biochemical and local failure in patients with distended rectum on the planning CT for prostate cancer radiotherapy. Int J Radiat Oncol Biol Phys 2005;62:965–973.

59 Kupelian PA, Willoughby TR, Reddy CA et al. Impact of image guidance on outcomes after external beam radiotherapy for localized prostate cancer. Int J Radiat Oncol Biol Phys 2008;70:1146–1150.

60 Rubens DJ, Yu Y, Barnes AS et al. Image-guided brachytherapy for prostate cancer. Radiol Clin North Am 2006;44:735–748, viii–ix.

61 Acher PL, Morris SL, Popert RJ et al. Permanent prostate brachytherapy: A century of technical evolution. Prostate Cancer Prostatic Dis 2006;9:215–220.

62 Pasteau O, Degrais P. De l'emploi du radium dans les cancers de la prostate. J Urol (Paris) 1913;4:341–345.

63 Aronowitz JN. Benjamin Barringer: Originator of the transperineal prostate implant. Urology 2002;60:731–734.

64 Whitmore WF Jr, Hilaris B, Grabstald H. Retropubic implantation of iodine 125 in the treatment of prostatic cancer. Trans Am Assoc Genitourin Surg 1972;64:55–57.

65 Acher PL, Dasgupta P, Popert R. Improving prostate brachytherapy by developing image guidance. BJU Int 2007;99:241–243.

66 Holm HH, Juul N, Pedersen JF et al. Transperineal ^{125}iodine seed implantation in prostatic cancer guided by transrectal ultrasonography. J Urol 1983;130:283–286.

67 Grimm PD, Blasko JC, Sylvester JE et al. 10-year biochemical (prostate-specific antigen) control of prostate cancer with (125)I brachytherapy. Int J Radiat Oncol Biol Phys 2001;51:31–40.

68 Citrin D, Ning H, Guion P et al. Inverse treatment planning based on MRI for HDR prostate brachytherapy. Int J Radiat Oncol Biol Phys 2005;61:1267–1275.

69 Fuller DB, Jin H, Koziol JA et al. CT-ultrasound fusion prostate brachytherapy: A dynamic dosimetry feedback and improvement method. A report of 54 consecutive cases. Brachytherapy 2005;4:207–216.

70 Kaplan ID, Meskell P, Oldenburg NE et al. Real-time computed tomography dosimetry during ultrasound-guided brachytherapy for prostate cancer. Brachytherapy 2006;5:147–151.

71 Mizowaki T, Cohen GN, Fung AY et al. Towards integrating functional imaging in the treatment of prostate cancer with radiation: The registration of the MR spectroscopy imaging to ultrasound/CT images and its implementation in treatment planning. Int J Radiat Oncol Biol Phys 2002;54:1558–1564.

72 Pouliot J, Kim Y, Lessard E et al. Inverse planning for HDR prostate brachytherapy used to boost dominant intraprostatic lesions defined by magnetic resonance spectroscopy imaging. Int J Radiat Oncol Biol Phys 2004;59:1196–1207.

73 Reed DR, Wallner KE, Narayanan S et al. Intraoperative fluoroscopic dose assessment in prostate brachytherapy patients. Int J Radiat Oncol Biol Phys 2005;63:301–307.

74 Reynier C, Troccaz J, Fourneret P et al. MRI/TRUS data fusion for prostate brachytherapy. Preliminary results. Med Phys 2004;31:1568–1575.

75 DiBiase SJ, Hosseinzadeh K, Gullapalli RP et al. Magnetic resonance spectroscopic imaging-guided brachytherapy for localized prostate cancer. Int J Radiat Oncol Biol Phys 2002;52:429–438.

76 D'Amico AV, Cormack R, Tempany CM et al. Real-time magnetic resonance image-guided interstitial brachytherapy in the treatment of select patients with clinically localized prostate cancer. Int J Radiat Oncol Biol Phys 1998;42:507–515.

77 D'Amico AV, Moul JW, Carroll PR et al. Surrogate end point for prostate cancer-specific mortality after radical prostatectomy or radiation therapy. J Natl Cancer Inst 2003;95:1376–1383.

78 Zelefsky MJ, Yamada Y, Cohen GN et al. Intraoperative real-time planned conformal prostate brachytherapy: Post-implantation dosimetric outcome and clinical implications. Radiother Oncol 2007;84:185–189.

79 Dubois DF, Prestidge BR, Hotchkiss LA et al. Intraobserver and interobserver variability of MR imaging- and CT-derived prostate volumes after transperineal interstitial permanent prostate brachytherapy. Radiology 1998;207:785–789.

80 Crook J, Milosevic M, Catton P et al. Interobserver variation in postimplant computed tomography contouring affects quality assessment of prostate brachytherapy. Brachytherapy 2002;1:66–73.

81 Bice WS Jr, Prestidge BR, Grimm PD et al. Centralized multiinstitutional postimplant analysis for interstitial prostate brachytherapy. Int J Radiat Oncol Biol Phys 1998;41:921–927.

82 DiBiase SJ, Wallner K, Tralins K et al. Brachytherapy radiation doses to the neurovascular bundles. Int J Radiat Oncol Biol Phys 2000;46:1301–1307.

83 Crook JM, Potters L, Stock RG et al. Critical organ dosimetry in permanent seed prostate brachytherapy: Defining the organs at risk. Brachytherapy 2005;4:186–194.

84 Bentzen SM. Theragnostic imaging for radiation oncology: Dose-painting by numbers. Lancet Oncol 2005;6:112–117.

85 Chao KS, Bosch WR, Mutic S et al. A novel approach to overcome hypoxic tumor resistance: Cu-ATSM-guided intensity-modulated radiation therapy. Int J Radiat Oncol Biol Phys 2001;49:1171–1182.

86 Sullivan DC. Imaging as a quantitative science. Radiology 2008;248:328–332.